Journal of Neuroscience Methods 201 (2011) 106–115

Contents lists available at ScienceDirect

Journal of Neuroscience Methods

journal homepage: www.elsevier.com/locate/jneumeth

A novel telemetry system for recording EEG in small animals

Pishan Chang[a,1], Kevan S. Hashemi[b,*], Matthew C. Walker[a]

[a] Department of Clinical and Experimental Epilepsy, UCL Institute of Neurology, University College London, London WC1N 3BG, United Kingdom
[b] OpenSource Instruments Inc., Watertown, MA 02472, United States

ARTICLE INFO

Article history:
Received 22 December 2010
Received in revised form 14 July 2011
Accepted 19 July 2011

Keywords:
Electroencephalography
Epilepsy
Wireless telemetry
Rats
Open source

ABSTRACT

It has become increasingly evident that continuous EEG monitoring is necessary to observe the development of epilepsy in animals, and to determine the effect of drugs on spontaneous seizures. Telemetric recording systems have been increasingly used to monitor EEG in freely moving animals. One challenge faced by such systems is to monitor frequencies above 80 Hz continuously for weeks. We present an implantable, 2.4-ml, telemetric sensor that can monitor EEG at 512 samples per second for eight weeks in a freely moving animal. With minor modifications, the same transmitter can operate at higher sample rates with a proportional decrease in operating life. Signal transmission is through bursts of 915-MHz radio power. The burst transmission and several other novel techniques reduce the transmitter's power consumption by two orders of magnitude while allowing 8 transmitters to share the same recording system. The use of radio-frequency transmission permits digitization within the sensor to sixteen-bit resolution, thus eliminating transmission-generated signal noise. The result is a signal with dynamic range 9 mV, bandwidth 160 Hz, input noise 12 μV, and AC power interference less than 1 μV. All circuit diagrams are open-source. Data acquisition takes place over the Internet using open-source software that works on multiple operating systems. The resulting system permits long-term, continuous, monitoring of EEG signals, therefore providing continuous and reliable data upon which to base studies of epilepsy in freely moving animals.

1. Introduction

Epilepsy is the propensity to have spontaneous seizures. Seizures are transient symptoms associated with abnormal, excessive, or synchronous neuronal activity in the brain. They can cause a variety of temporary and debilitating changes in perception and behavior. Epilepsy is one of the most common serious neurological diseases, affecting 0.5–1% of the population (Sander and Shorvon, 1996). The drugs that we presently use to treat epilepsy are symptomatic; they prevent seizures rather than modify the condition. Furthermore, these drugs treat only 70% of people successfully (Kwan and Brodie, 2000). More effective treatments and disease-modifying treatments are urgently needed (Walker et al., 2002). Acquired and genetic animal models of spontaneous seizures have been developed to investigate the mechanisms underlying the development of epilepsy (epileptogenesis) and to evaluate the effect of drugs on epileptogenesis and spontaneous seizures (Schmidt and Rogawski, 2002). It has become increasingly apparent that continuous electroencephalogram (EEG) is required to observe the effects of treatment and for mapping the development of epilepsy (Williams et al., 2009), especially because ictal EEG activity can precede the earliest observable changes in behavior (Lieb et al., 1976; Litt et al., 2001).

Monitoring physiological signals in a rodent can be achieved by running wires from the animal's body to amplifiers and recording equipment outside the cage. Such "tethered systems" have been successful in long-term monitoring of EEG and have permitted the correlation of EEG with behavior. Unlike battery-operated systems, tethered systems can provide the power necessary for long-term recordings with multiple electrodes and high sampling rate.

There are, however, several disadvantages to tethered systems. Being tethered by wires can cause some distress to the animals, a potential source of experimental artifact and inter-animal variability (Kramer et al., 2001). Whenever the animal moves, the tethering wires also move. These movements interact with electrostatic fields in the animal's cage, resulting in transient noise known as "movement artifact". This noise can be difficult to differentiate from biological signals. Moreover, any separation between the wires causes them to detect magnetic fields generated by nearby alternating currents, resulting in 50-Hz or 60-Hz noise termed "mains

Abbreviations: SE, status epilepticus; EEG, electroencephalogram; LWDAQ, long-wire data acquisition driver; SCT, subcutaneous transmitter.

* Corresponding author. Tel.: +1 781 736 2819.
E-mail address: hashemi@opensourceinstruments.com (K.S. Hashemi).
[1] Present address: Centre for Biomedical Sciences, School of Biological Sciences, Royal Holloway University of London, Egham TW20 0EX, United Kingdom.

0165-0270/$ – see front matter © 2011 Elsevier B.V. All rights reserved.
doi:10.1016/j.jneumeth.2011.07.018

hum". The animal's body must be connected with a low-impedance wire to the ground potential of the recording equipment, or else variation in the animal's body potential will corrupt or saturate the signal. However, this ground wire will itself add mains hum and movement artifacts to the signal.

A sensor implanted within an animal's body can avoid the electrical noise of a tethered system. The electrodes, wires, and sensor are immersed in the same conducting animal body. They are therefore unaffected by external electrostatic fields, and generate far fewer movement artifacts. The leads run close together and are short. They generate far less mains hum. Because the device is battery-powered, no separate low-impedance ground connection is required between the sensor and the animal's body. The animal can move freely about its cage, improving its comfort during long-term recordings.

There are, however, several difficulties to overcome when designing an implantable sensor. One is the problem of providing power to the sensor. Using an alternating magnetic field to convey power into the sensor will corrupt the recorded signal with currents induced in the electrode leads. A low-noise, implantable sensor must obtain its power from a battery alone. The sensor must be small enough to fit comfortably beneath the skin of the animal in which it is to be used. For long-term experiments, the material surrounding the sensor must be biocompatible, fatigue-resistant, and waterproof. The leads themselves must be flexible and resistant to corrosion. If we are to view the signal while the sensor is implanted, the sensor must transmit its samples out of the animal's body to some form of recording equipment. Given the evidence of longer-term progression in animal models (Kadam et al., 2010), the sample transmission must consume as little power as possible so that the battery can keep the sensor running for weeks at a time.

Reports by experimenters working with existing EEG telemetric systems indicate significant restrictions to their application (Mumford and Wetherell, 2001; Obeid et al., 2004; Williams et al., 2006). Their operating range is usually far shorter than is convenient. The sample rate is either too low to provide accurate recordings above 80 Hz (Bragin et al., 2005; Traub et al., 2001; Worrell et al., 2004) or the operating life is too short for long-term monitoring (Lapray et al., 2008).

Another problem with existing telemetry systems is the lack of technical specifications provided by their manufacturers, including fundamental properties such as sampling rate of the sensor, the noise present on the input, the nature of the anti-aliasing filters, and the input impedance of the amplifier (see Table 1). Furthermore, many telemetry systems require proprietary software. This software can be expensive and usually runs on a single operating system. Sometimes, the software applies unknown processing to the acquired signals.

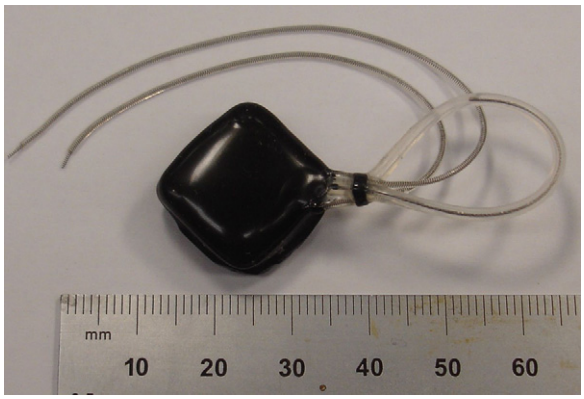

Fig. 1. The subcutaneous transmitter A3013A, showing coiled wire leads and loop antenna.

We have therefore designed an open-source telemetry system with freely available circuit diagrams, complete performance specifications, and free software that can run on multiple operating systems. Here we describe this system and the features that permit high sample rate, low noise, and long operating life. We describe sensor encapsulation and lead manufacture. We go on to demonstrate reliable radio reception and transmitter performance during normal behavior and induced seizures.

2. Materials and methods

2.1. System overview

The Subcutaneous Transmitter (SCT) system permits recordings from animals housed together or separately. The transmitters are implanted beneath the skin of the animals. Fig. 1 shows our prototype A3013A transmitter. Table 1 presents the A3013A's electrical and mechanical specifications. The table also presents the specifications of the newer A3019D transmitter, which provides twice the battery life for the same volume and sample rate. The A3019A is half the volume of the A3013A, with half the battery life, and is designed for use in mice. All three transmitters provide only one input channel. A loop of stranded, stainless steel wire encased in a silicone tube acts as the transmitting antenna. Two stainless steel springs coated with silicone act as the electrode leads.

Fig. 2 presents the layout of a typical SCT system. Antennas outside the animal cages receive the transmitter samples. The SCT transmission uses radio waves of frequency 905–915 MHz. Faraday enclosures isolate each SCT system from external interference and make it possible for many SCT systems to operate in the same laboratory without interfering with one another. Each faraday enclosure

Table 1
Comparison with existing devices. The manufacturers are OpenSource Instruments Inc. (OSI), Data Science International (DSI), Telemetry Research (TR), NewBehavior, and Triangle Biosystems International (TBSI). Entries marked "unknown" are those for which we were unable to obtain any specific values from the manufacturer.

Device	A3013A	A3019D	CAF40	TR40B	Neurologger	S05010
Manufacturer	OSI	OSI	DSI	TR	NewBehavior	TBSI
Type	Implant RF	Implant RF	Implant magnetic	Implant RF	Headset logger	Headset RF
Channels	1	1	1	1	4	5
Volume	2.4 ml	2.2 ml	4.5 ml	7.2 ml	1.3 ml	0.8 ml
Sample rate	512 SPS	512 SPS	1 kSPS	2 kSPS	500 SPS	50 kSPS
Bandwidth	160 Hz	160 Hz	200 Hz	Unknown	100 Hz	7 kHz
Input noise	12 μV	12 μV rms	5 μV rms	Unknown	Unknown	Unknown
Input range	9 mV	20 mV	20 mV	4 mV	1.5 mV	4 mV
Input impedance	10 MΩ	10 MΩ	300 kΩ	Unknown	>10 MΩ	11 MΩ
ADC precision	16-bit	16-bit	No ADC	12-bit	10-bit	Unknown
Operating life	9 weeks	19 weeks	26 weeks	12 h	60 h	3.5 h
Battery re-use	No	No	Factory replace	User recharge	User replace	User recharge
Supported operating systems	Windows Linux Macos	Windows Linux Macos	No software needed	No software needed	Windows	Windows

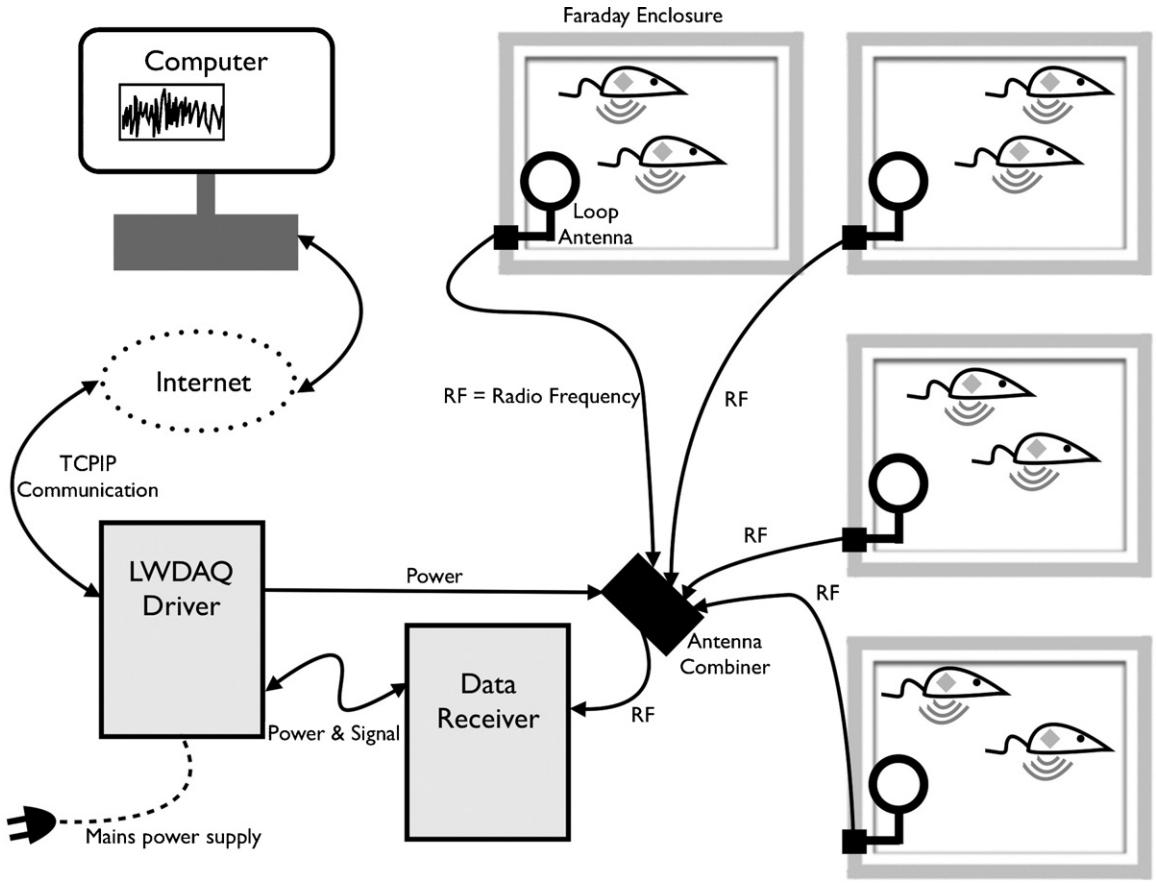

Fig. 2. Schematic of the main components of the telemetric system. Four faraday cages are connected via an antenna combiner to the data receiver and then to a LWDAQ driver which connects via the Internet to a computer.

contains its own antenna and one or more animal cages. Up to four antennas are connected to an Antenna Combiner (A3021B), whose output is connected to a Data Receiver (A3018C). The data receiver demodulates, decodes, and records the SCT signals. A single data receiver can record from up to 14 transmitters, but in the experiments we describe below, we record from only 8 transmitters.

The data receiver connects to a Driver with Ethernet Interface (A2037E), which provides power to the data receiver and antenna combiner. The driver provides an interface between the Internet and the data receiver. It derives its own power from a wall socket.

A data acquisition computer somewhere on the Internet runs our open-source data-acquisition software. The computer downloads the transmitter signals and stores them on its hard drive in archive files. At the same time, the computer can display and analyze the signals, or it can display and analyze previously recorded signals.

2.2. Transmitter electronics

Fig. 3 gives the circuit diagram of the A3019 transmitter. This circuit is simpler, but functionally equivalent to that of the A3013A. The two electrode leads connect to the X terminals. These terminals are connected by a 100-nF capacitor in series with a 10-MΩ resistor, which together define the transmitter's input impedance.

The X− input is connected directly to the amplifier's ground potential. Here we see one of the great advantages of the battery-operated amplifier. The entire transmitter is isolated from the animal's body, except at the two electrodes. The capacitance between the transmitter and the animal's body is roughly 10 pF. At 160 Hz and below, this capacitance has impedance greater than 100 MΩ, and is therefore insignificant compared to the transmitter's 10-MΩ input impedance. Thus we obtain a near-perfect differential input using two leads with no need for a low-impedance ground.

The difference between X+ and X− is amplified in two stages. The total gain depends upon resistor R10 in the first stage (Fig. 4). The A3019A and A3019D provide a total gain of 100. The A3013A provides a total gain of 300. The first stage provides one pole of a three-pole, low-pass, anti-aliasing filter, while the second stage provides the second and third poles. In the A3019A, which samples at 512 SPS, the amplifier and filter provide a gain of 100 at 160 Hz, 10 at 256 Hz, and 1 at 512 Hz. Signals above 256 Hz, which would be converted into aliasing noise by sampling at 512 SPS, are attenuated by at least a factor of ten. The filter reduces their contribution to power spectra by at least two orders of magnitude.

The amplified and filtered signal passes to U5, a 16-bit ADC (analog to digital converter). Programmable logic chip U6 controls and reads out the converter. The logic chip receives its sample timing from a 32.768-kHz oscillator, U4. At each sample instant, the logic chip turns on its internal ring oscillator to generate a 5-MHz transmission clock. It reads out the ADC bits, and initiates the next conversion. Component U7 is a voltage-controlled oscillator (VCO) that the transmitter uses as a radio transmitter. Resistors R4–R8 create a five-bit DAC (digital to analog converter) to drive the tuning input of U7. The DAC allows the logic chip to modulate the VCO output from 905 MHz to 915 MHz to indicate binary zeros and ones respectively. The output of U7 connects directly to the antenna.

The transmitter's on–off switch is U1, a Hall-Effect sensor. A magnet brought near the transmitter switches the state of latch U2. If the transmitter is off, it will turn on and vice versa. The A3013A

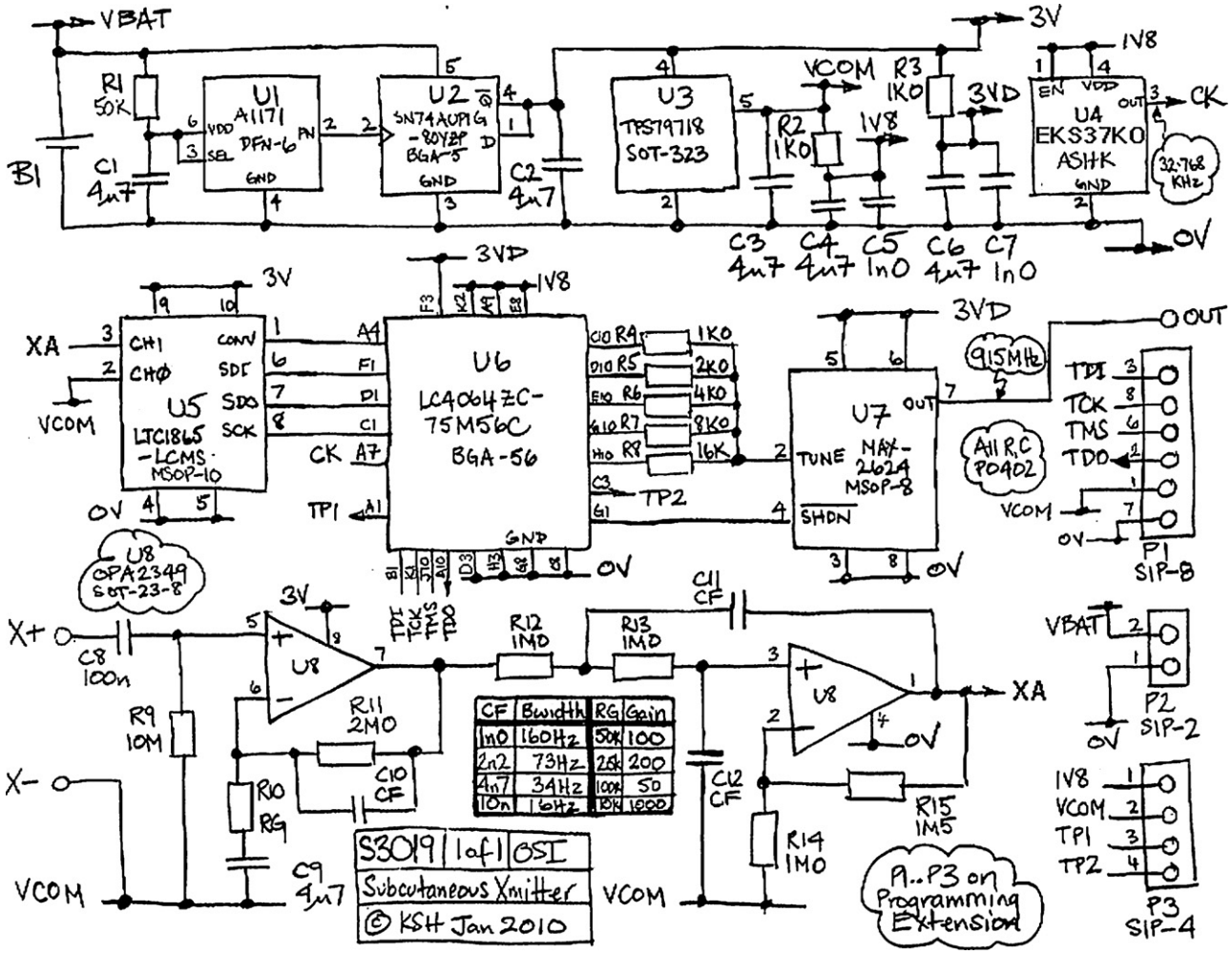

CF	Bwidth	RG	Gain
1n0	160Hz	50K	100
2n2	73Hz	25K	200
4n7	34Hz	100K	50
10n	16Hz	10K	1000

Fig. 3. Circuit diagram of the subcutaneous transmitter A3019A.

transmitter used a reed relay instead of a Hall-Effect sensor. The reed relay worked well, but was far less sensitive.

The transmitter transmits information for only 10 μs during each sample period. These bursts contain the transmitter identification bits, the ADC bits, and some error-checking bits. When the sample rate is 512 SPS, each transmitter transmits for only 0.5% of the time. The transmitter's current consumption is 12 mA when transmitting, but only 20 μA for the remaining 99.5% of the time. Thus its average current consumption is only 80 μA. Equipped with a 125 mA-h, 3-V lithium battery, the A3013A will run for 1500 h (9 weeks). With a 48 mA-h battery, the A3019A runs for 600 h. The A3019D's 255 mA-h battery provides operating life of over 3200 h. If we increase the sample rate to 2048 SPS, the A3019D will run for 980 h. If we were to add a second channel to the A3019D circuit and run both channels at 512 SPS, the two-channel device would run for 1800 h. In the off state, the A3019 transmitters consume only 5 μA, so that the A3019D can sit on the shelf for six years before it exhausts its battery. A six-month delay between building the transmitter and implantation will reduce the operating life by less than 10%.

Other commercially available radio-frequency transmitters do not use burst transmission, but instead transmit continuously using off-the-shelf transceiver chips. Their current consumption is around 12 mA, which is why their battery life tends to be one hundred times shorter than that of our transmitters for the same sample rate. One advantage of using off-the-shelf transceiver chips is that they provide two-way communication between the transmitter and the receiver. Our transmitters provide only one-way communication.

Another advantage offered by off-the-shelf transceivers is that their transmissions are less vulnerable to multi-path interference. Multi-path interference occurs when the line-of-sight signal between the transmitter and the antenna combines with a reflected signal to produce a signal that is too small to be detected. Off-the-shelf transceiver chips operate in a narrow frequency band, such as 915.0–915.1 MHz, while our burst transmissions occupy 905–915 MHz. Multi-path interference occurs at discrete frequencies for any given transmitter orientation and position. The probability that one of these discrete frequencies lies within the 10-MHz bandwidth of our burst transmission is one hundred times greater than for transmissions that occupy a 0.1-MHz bandwidth. Nevertheless, the SCT system almost entirely overcomes multi-path interference through the use of loop antennas that transmit and receive in all directions, thereby reducing the probability that a reflected signal will be as strong as the line-of-sight signal.

Another potential problem for the SCT system arises when two transmitters select the same 10-μs interval for transmission. The two radio frequency bursts will interfere with one another. If both are of similar strength, both will be lost. If the internal clocks of two transmitters coincide with one another, such "collisions" could be systematic for minutes at a time. To avoid systematic collisions, each transmitter displaces its transmission burst by a random length of time derived from the bottom four bits of its most-recent sixteen-bit sample. These four bits are dominated by electronic

Fig. 4. Faraday enclosure with one animal cage. The enclosure will accommodate two such cages.

noise. These random disturbances allow eight transmitters to share the same antenna with an average loss of only 5% due to collisions. A randomly distributed 5% loss is easy to correct in signal reconstruction.

2.3. Transmitter encapsulation

At the start of our development, we dipped the transmitter circuit in silicone dispersion a few times to provide it with an inert, waterproof coating. But this process leaves air bubbles within the silicone, trapped between the battery and the circuit board. When we shipped the transmitters by air from Boston to London, these bubbles expanded at altitude and burst the coating. After implantation, water leaked through the coating and damaged the transmitters within a matter of days.

We switched to a two-stage coating process. In the first stage we encapsulate the transmitter and battery in epoxy. Before the epoxy cures, we place the transmitter in a vacuum to expand the trapped air bubbles, causing them to emerge from within the transmitter. When we remove the vacuum, the epoxy is drawn into the transmitter interior to fill the internal spaces. After the epoxy has cured, we apply three coats of silicone to obtain an inert, rugged outer coating. This two-stage encapsulation endures vacuum indefinitely and implantation for at least eight weeks without any apparent damage.

2.4. Electrode leads

We needed electrode leads that could survive the repetitive strain of long-term implantation. Leads that run beneath the skin of a rat's neck will be flexed first one way and then another every time the rat moves its head from side to side. This flexing is not only lateral, but also longitudinal, because the leads become fixed in place by body tissue as the animal recovers from surgery. We estimate that the leads must endure a million cycles of bending and stretching during a two-month implantation.

We first tried PVC-insulated, stranded copper wires. Within a day or two, the transmitter would fail. Body fluid penetrated the porous PVC insulation. Once between the copper strands, fluid traveled by capillary action along the length of the leads. With our original silicone coating, fluid was free to spread from the base of the leads across the circuit board, where it would immediately disrupt the amplifiers and eventually drain the battery. Our epoxy encapsulation does not permit fluid to spread from the base of the leads. Within a week of implantation, however, the fluid corrodes the copper strands, causing the entire wire to break.

We tried Teflon-insulated, solid, stainless steel wires. These do not conduct body fluids by capillary action because there are no spaces along which fluids may travel. But they break by fatigue within a few days to a few weeks. So we tried Teflon-insulated, stranded, stainless steel wires. These conduct fluids by capillary action, but are far more resistant to corrosion than copper, and our epoxy encapsulation blocked fluids carried within the wires. The stranded steel wires broke by fatigue within a few weeks also, with the exception of the largest size we tried, one with seven 100-μm diameter strands. This wire was so stiff that it caused infection and discomfort in the animals.

We therefore turned to small-diameter stainless steel springs. We found two companies (Motion Dynamics Corporation and Century Spring Corporation) that can manufacture closed-form springs 75 mm long with outer diameter 500 μm using 100-μm stainless steel wire. We take one such spring and stretch it so that it becomes a helix of stainless steel 150 mm long. We coat the helix by hand five times with silicone dispersion to create a lead that is flexible in every direction, including along its own length. There are no gaps between the spring and the insulation, so there is no possibility of body fluids traveling down the lead. These insulated springs proved to be immune to fatigue and corrosion during eight-week implantations.

2.5. Transmitting antenna

The antenna itself is a loop of wire protruding from the transmitter body, rather than something more compact mounted on the circuit board. The efficiency of any antenna is affected by the dielectric constant of the material that surrounds it. Compact antennas, such as those we can make out of zig-zag copper traces, or coiled wires, are particularly sensitive to their surroundings. The dielectric constant of water is eighty times that of air, so the ideal length of any antenna will be nine times less when immersed in water. The efficiency of the compact antennas we tried varied by a factor of one hundred as we clasped them in a fist, implanted them in an animal body, left them out in air, or immersed them in saltwater. Our 50-mm loop antenna's efficiency, however, is far less variable. It is most efficient when implanted just beneath the skin of a rat, but it works well in air, in a fist, or immersed completely in water.

Furthermore, compact antennas tend to transmit almost all their power in a single plane, such as the plane perpendicular to their length. In other directions, they emit hardly any power. We wanted our antenna to transmit as uniformly as possible in all directions, so that reflected signals would rarely be as powerful as the line-of-sight signal. Of all the antenna shapes we tested, a simple loop provided the smallest variation in transmitted power with direction.

The loop antenna must be flexible to endure repetitive strain in the animal, but we cannot construct it out of a helical steel wire such as we use for our electrode leads. The length of the antenna conductor would have to include the turns of the helix. Helical antennas are compact but their efficiency is a strong function of environment and orientation. At the same time, the fatigue suffered by the antenna is not as severe as that suffered by the electrode leads. The antenna is shorter and is fastened to the transmitter at both ends. So we construct the antenna using a conductor made of forty-nine separate strands of stainless steel wire. Its outer diameter is 360 μm. Enclosed in a pre-formed silicone tube, the antenna survives eight weeks of implantation with no apparent damage.

2.6. Faraday enclosures

The faraday enclosures are made out of aluminum angle brackets for the frame, aluminum sheets for the lid, base, and back wall, and steel fabric for the sides and front. Beneath the lid is a square

of microwave-absorbing foam to dampen radio-frequency oscillations. Fig. 4 shows a prototype faraday enclosure with all sides made of steel fabric.

Because each enclosure is isolated from the outside world, it must have its own antenna. The SCT system shown in Fig. 2 connects four enclosures to a single data receiver. Because of the isolation offered by the faraday enclosures, another SCT system of four faraday enclosures could share the same laboratory, Thus the faraday enclosures provide two functions. They keep out radio-frequency interference and they isolate one SCT system from another, thus increasing the number of animals that can be monitored simultaneously.

2.7. Data acquisition

Data acquisition takes place over the Internet or over a local area network. The Data Receiver connects to a LWDAQ Driver with Ethernet Interface and the data acquisition computer runs the LWDAQ Software. The acronym "LWDAQ" stands for Long Wire Data Acquisition. There are no long wires in the SCT system, but there were long wires in the ATLAS experiment at CERN for which the LWDAQ hardware and software were designed by Brandeis University, Boston, USA. The LWDAQ system provided us with a ready-made, open-source foundation upon which to build the SCT system. The LWDAQ Software provides a Recorder Instrument to download data from a Data Receiver and a Neuroarchiver Tool to record and analyze transmitter signals.

2.8. Data analysis

At the heart of the data acquisition software is a TclTk interpreter. TclTk is a scripting language that allows files, TCPIP sockets, images, graphical user interfaces, and text strings to be manipulated with simple commands (Welch, 1997). The Neuroarchiver records transmitter signals in archive files without any pre-processing. It also plays back previously recorded, or freshly recorded data, displaying the signals on the computer screen along with their frequency spectra, as calculated by a discrete Fourier transform. Playback intervals can be varied from a fraction of a second to many seconds.

The archive files contain a list of samples received from all active transmitters along with clock messages generated by the data receiver. During playback, the Neuroarchiver applies a reconstruction algorithm to produce a fixed number of samples per second for each active transmitter. If all samples are present in the archive, no alteration of the original signal takes place. But if a sample is missing, as a result of multi-path interference or a collision between transmitters, the reconstruction inserts a substitute sample whose value is equal to that of the most-recently received sample from the same transmitter. By this means, the loss of 20% of samples, distributed at random, can be almost entirely overcome at the time of playback.

During playback, a user-defined TclTk "processor script" produces a single line of text that summarizes the characteristics of the signals during each playback interval. The user might choose to record the power in several frequency bands for each transmitter. The Neuroarchiver stores these text lines on disk to produce "characteristics files". We analyze the characteristics files at a later time with a TclTk "analysis script", also written by the user. Seizure detection might proceed by detecting sustained periods of high power in the 2–20 Hz band as recorded in the characteristics files.

Analyzing the characteristics files is fast, while processing the raw data is slow. Each 512 SPS transmitter produces 2 kB of data per second. Each sample consists of four bytes: a transmitter identifier, the sixteen-bit sample, and a timestamp. Two months of recording from eight transmitters produces over 100 GB of data. Re-processing this data means re-calculating the Fourier transform of all the playback intervals. A single desktop computer will take a week to do the job. But a cluster of computers can get it done in less than a day. The Neuroarchiver will run in a no-graphics mode that allows batch processing by a Linux cluster.

2.9. Animal surgery

We conducted all experiments in accordance with the UK Home Office regulations under the Animal Scientific Procedures Act, 1986. Male Sprague–Dawley rats weighing 200–300 g were housed individually in standard plastic cages measuring 42 cm × 26 cm × 20 cm under a 12 h light–dark cycle. The room temperature was maintained at 24–25 °C and relative humidity at 50–60%. Standard rodent food and tap water were provided.

We performed surgery in deeply anesthetized animals, maintained with 2% isoflurance in O_2, at a flow rate of 2 L/min using a stereotaxic frame with heating pad (David Kopf Stereotaxic Frame). We placed three screws in the skull: two rostral to bregma and one caudal. We placed the transmitter beneath the skin on the back of the animal and secured it with a suture. We threaded the electrode leads under the skin to the exposed skull. We connected the X− wire to the two anterior screws and held the X+ wire in place extradurally with the caudal screw. The whole assembly was held in place with dental cement (Simplex Rapid, Acrylic Denture Polymer, UK). We allowed the animals to recover for a period of 7 days after surgery.

2.10. Status epilepticus

We administered kainic acid (Sigma) at a dose of 10 mg/kg by intraperitoneal injection. We watched the animals for behavioral changes and rated the severity of observed seizures based on the Racine scale (stage 1, mouth and facial movements; stage 2, head nodding and more serve facial and mouth movements such as jaw-opening; stage 3, forelimb clonus; stage 4, rearing and bilateral forelimb clonus; stage 5, rearing and falling, with loss of postural control, full motor seizure) (Racine, 1972). We terminated the seizures one hour after the rats reached stage 5 by administering pentobarbitol (30 mg/kg intraperitoneally). We injected saline subcutaneously to aid the animal's recovery.

3. Results

3.1. Health of the animals

There were no post-surgical infections around the transmitter in 22 animals for periods up to 3 months. Rats were less active in the 2–3 days after surgery which is consistent with previous observations (Goecke et al., 2005), but thereafter there was no evidence of discomfort or animal distress, and the implanted transmitters did not impede animal movement. All animals were able to groom, eat, drink, move and curl up to sleep freely.

3.2. Reliability of the sensor

At the end of an eight-week experiment with eight transmitters implanted in active rats, the transmitter body, antenna, and electrode leads showed no sign of wear, corrosion, or fatigue.

During an eight-week experiment with eight transmitters implanted in eight animals in four faraday enclosures at the top of a building in the center of London, UK, we received an average of 95% of samples from all transmitters. Every hour or so, reception from a random transmitter dropped below 20% for ten or twenty seconds. In other tests, we confirmed that such short-term losses are the result of signal cancellation by reflected radio waves. Both

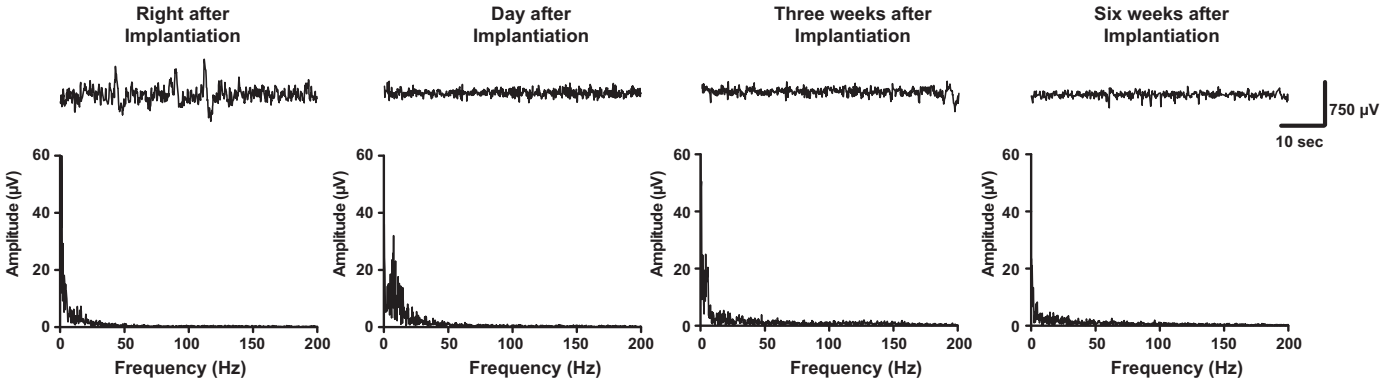

Fig. 5. Examples of EEG recordings from the cortex of freely moving adult rats up to six weeks after implantation. The upper plots show voltage versus time. The lower plots show amplitude versus frequency from the discrete Fourier transform.

animals in the enclosure must remain perfectly still for such losses to occur. We have not observed such signal loss during an epileptic seizure. The sustained 5% loss is what we expect from signal collisions among eight transmitters.

3.3. Long-term EEG recording

We implanted ten A3013A transmitters in ten separate rats. Immediately after implantation, each rat was caged individually. We started EEG recording immediately after surgery, and continued recording for 8 weeks or longer (Fig. 5, $n = 10$). The EEG recordings demonstrated normal brain activity shown over time and frequency domains (Fig. 5). Immediately after surgery, while the rats were recovering from anesthesia, the EEG demonstrated a burst suppression pattern consisting of high-amplitude activity interrupted by relatively low amplitude activity (Hartikainen and Rorarius, 1999) (Fig. 5).

Fig. 6A shows a typical baseline EEG recording from an active animal one week after surgery and shortly before kainic acid injection. The amplitude of the EEG signal is 80-µV rms. During the entire eight weeks of the experiment, there were minimal muscle or movement artifacts in the EEG signals.

We treated all ten rats with kainic acid (10 mg/kg, i.p.) seven days after implantation. Injection of kainic acid induced convulsive status epilepticus. One hour after reaching convulsive (stage 5) seizures, we administered pentobarbital (30 mg/kg ip) to stop seizure activity and improve survival. Following kainic acid injection, we observed characteristic EEG and clinical seizures progression. Occasional bursts of high frequency activity occurred with increasing amplitude at mean time 17 ± 4 min after the injection, without any obvious accompanied behavioral changes (Figs. 6B and 7). The EEG we obtained during status epilepticus was free of movement artifacts, showing clear spikes even though the animals are convulsing (Fig. 6B).

The frequency spectrum of the EEG signal, which we obtain by fast Fourier transform in the Neuroarchiver program, demonstrated increasing amplitude at frequencies up to 60 Hz during stage 2 (Fig. 7C). Interictal spike activity persisted for the duration of the recordings. The behavioral seizures progressed to stage 3 (forelimb clonus) 52 ± 3 min after kainic acid injection. The EEG recording at this time demonstrated discontinuous bursts of spikes accompanied by an increase in the amplitude of the spikes to 400 µV as the seizure progressed (Fig. 7B and C). The behavioral seizure progressed to stage 4 (rearing and bilateral forelimb clonus) at 80 ± 6 min after kainic acid injection, and the amplitude of the spikes increased to 900 µV (Fig. 7B). The frequency spectrum demonstrated an increase in amplitude for frequencies up to 160 Hz, the limit of the transmitter's sensitivity (Fig. 7C). When seizure behavior reached stage 5 (rearing and failing, and full motor seizure) 92 ± 6 min after injection of kainic acid, the EEG recording showed continuous EEG spikes with amplitudes of up to 1500 µV (Fig. 7B). The EEG seizures and behavioral seizures ceased after

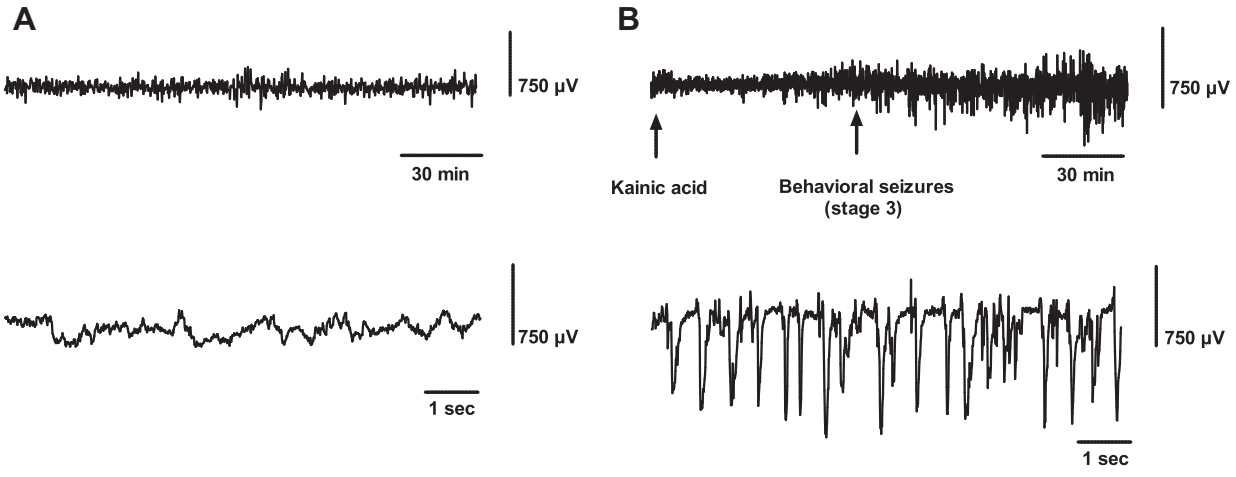

Fig. 6. Examples of EEG recordings from the cortex of adult rats in different states. (A) Examples of three-hour and ten-second of EEG recordings from the cortex of active adult rats. (B) Examples of three-hour and ten-second of EEG recordings from the cortex of adult rats with status epilepticus.

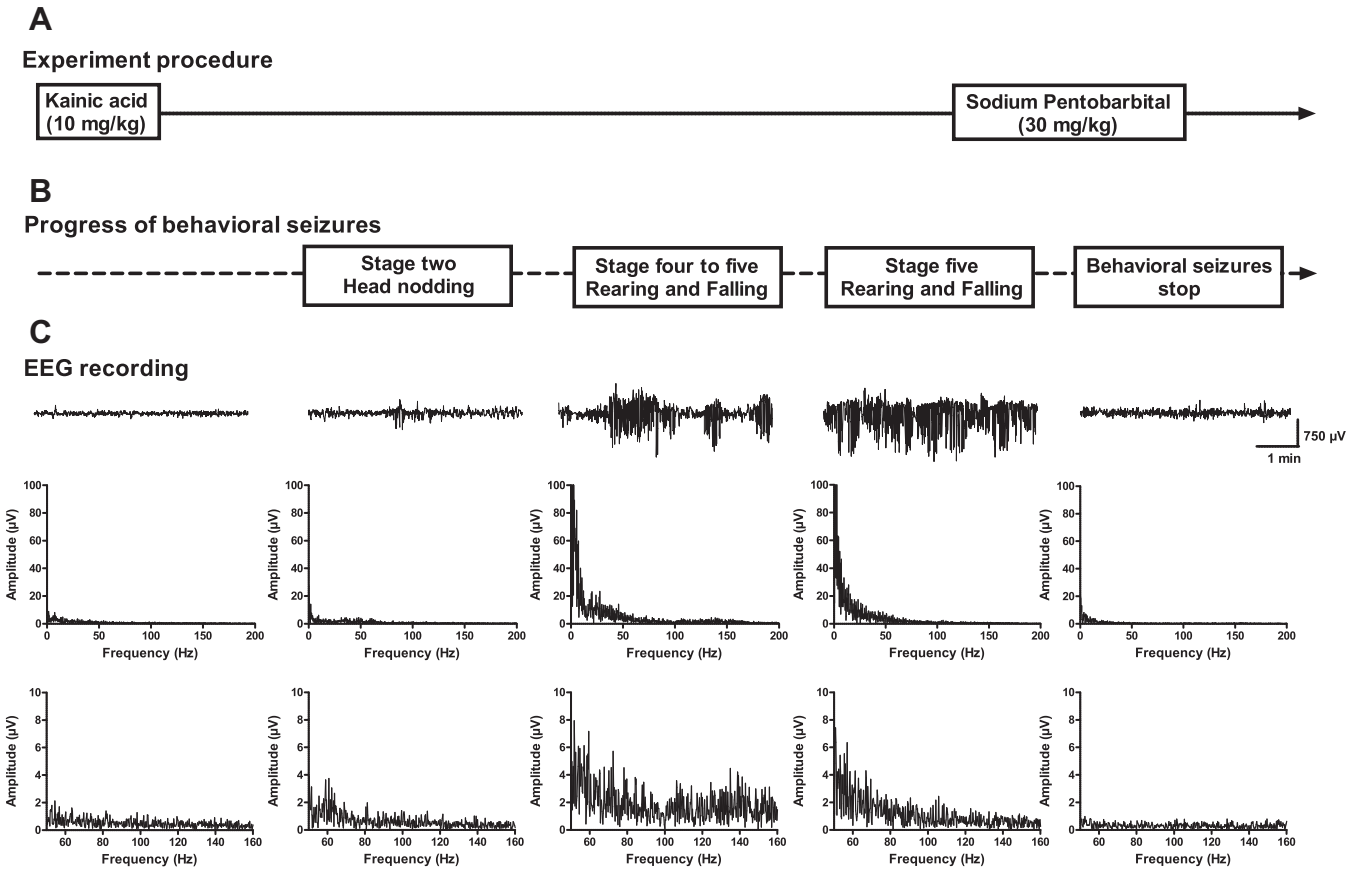

Fig. 7. Example of EEG activity recorded in status epilepticus rats induced by kainic acid. (A) The outline of experimental procedure. (B) The progress of behavioral seizures after administration of kainic acid. (C) The progress of EEG seizures after administration of kainic acid. The top row of plots in (C) show four-minute plots of voltage versus time. The middle rows show the EEG amplitude spectrum just before the onset of a seizure. The bottom row shows the EEG amplitude spectrum during a seizure.

administration with pentobarbital (30 mg/kg), at which time the frequency and amplitude of EEG returned to baseline level (Fig. 7B and C).

4. Discussion

We have demonstrated that the Subcutaneous Transmitter (A3013A) runs for over eight weeks, sampling continuously at 512 SPS, monitoring bandwidth 0.2–160 Hz in live animals. Its body, antenna, and electrode leads endure the repetitive stress caused by animal activity without any sign of fatigue. Its silicone coating is immune to the corrosive power of body fluids. With its volume of 2.4 ml, the A3013A fits comfortably beneath the skin of an adult rat.

Continuous EEG recording is needed to monitor the changes in spontaneous EEG seizures and motor seizures over time in order to elucidate mechanisms of epileptogenesis, and to study the effect of antiepileptogenic therapy designed to prevent the development of seizures (Grabenstatter et al., 2005; Hernandez et al., 2002) and therapies aimed at treating spontaneous seizures. Much of such work has been undertaken using tethered systems. However, tethering an animal can cause increased stress which could have adverse effects on hippocampal function and behavior (Wood et al., 2004). Moreover, stress can modify seizure susceptibility (Betts, 1992), perhaps explaining the observation that brief body restraint significantly lowers the seizure threshold for pentylenetetrazol-induced seizures in rodents (Swinyard et al., 1963). Tethering introduces noise and movement artifacts into an EEG signal. Nevertheless, tethered systems remain a useful method of recording EEG not least because they have the advantage of high sample rates from multiple channels without any limit imposed by battery life. The SCT system avoids tethering and so eliminates all its adverse effects. But the SCT sample frequency is constrained by its battery life. The A3019D transmitter, for example, will operate for 3200 h at 512 SPS, but only 980 h at 2 kSPS.

Other telemetry recording systems have been used for seizure monitoring (Williams et al., 2006, 2009), but have been limited by self-generated noise, indicating that EEG amplitudes must exceed 300 μV for accurate detection, an effect that is likely to impact particularly on higher biological frequencies, which tend to be of lower amplitude. The self-generated noise in the SCT transmitters is only 12 μV. In implanted transmitters, periodic noise induced by AC power is below the detectable limit of 1 μV. Similar systems have been limited to tens of hours of operation by battery life (Lapray et al., 2008). In order to extend battery life, sampling rates have been lowered in some systems to 100 SPS. The effective bandwidth of a signal sampled at 100 SPS will be less than 40 Hz. Our A3013A transmitter provides 160 Hz bandwidth with sample rate 512 SPS, and so it can measure activity in the 100–160 Hz band during status epilepticus induced by Kainic acid.

In Table 1 we compare the A3013A to four commercially available telemetry systems. The table also includes the A3019D, which replaces the A3013A for future experiments in rats. The A3019D provides the same performance as the A3013A, but with twice the battery life and a slimmer body. The A3019A, which we intend for experiments in mice, is not included in the table. The A3019A is identical to the A3019D, except its volume is 1.0 ml and its operating life is 4 weeks.

Data Science International (DSI) has long experience monitoring a variety of physiological parameters using wireless technology. The DSI system we present in Table 1 provides a single analog out-

put proportional to EEG voltage. Additional digitization hardware and analysis software must be purchased to provide seizure detection. The specification of the CAF40 transmitter is similar to that of our A3019D. Its battery life is 26 weeks compared to the A3019D's 19 weeks, while its volume is 4.5 ml compared to the A3019D's 2.2 ml. The CAF40s input impedance is only 300 kΩ, making it less suitable for use with high-impedance probes. Moreover, DSI uses a different transmission method based on the timing of magnetic pulses, requiring separate cages for each animal. These different forms of transmission may have their intrinsic advantages and disadvantages, but we have not directly compared the two systems experimentally.

The Neurologger records four channels of EEG directly to its own flash memory. It requires no transmission or reception, and so has been used on unconfined birds and animals. By infrared signaling, the user can introduce time marks into the recordings so that experimental events can be synchronized with recordings. Furthermore, the Neurologger includes an accelerometer, which allows the device to correlate EEG with physical activity. The main limitation of the Neurologger, for our purpose, is that it has only sixty hours of continuous operation, and is mounted outside the animal's body. Furthermore, it is not possible to examine the EEG signals while watching the animals, so the experimenter cannot detect problems with the system until after the experiment is complete.

The S05010 from TBSI provides 50 kSPS for recording the behavior of single neurons. But the device must be mounted outside the animal's body, and its battery life is only a few hours. The battery may be re-charged, but re-charging requires the user to plug a cable into the device.

The TR40B from Telemetry Research provides 2 kSPS for recording EEG. The output of their data acquisition system is an analog voltage, so the system requires no special software. The device may be implanted, but its volume is 7.2 ml, which is three times larger than we allowed for our A3013A. Furthermore, the TR40B runs for only twelve hours before it must be re-charged by placing the animal on a magnetic charging plate. By comparison, if we were to equip our A3019 circuit (Fig. 3) with a 4-ml lithium battery, and configure it to sample at 2 kSPS, the result would be a 5-ml device that would run continuously for 24 weeks.

The four manufacturers of competing systems listed in Table 1 declined to give us prices that we could compare publicly with our own. Readers may obtain quotations from the manufacturers directly.

All SCT printed circuit boards, bills of materials, drawings, assembly instructions, and software are available for free from the OSI website. In theory, any research institution can assemble its own SCT system. All the circuits and faraday enclosures are also available from OSI directly. The price of transmitters is 500 $US in quantity 10, and the price of a data acquisition system consisting of four faraday enclosures, one antenna combiner, one data receiver, and one driver is around 8000 $US. The sort of work we believe SCT users will find worth doing themselves is soldering new electrode screws onto the leads of transmitters that have been retrieved from deceased animals. Such work allows a single transmitter to take part in several experiments.

The Internet-based data acquisition implemented by the SCT system allows one computer to record transmitter signals and make them available over the local area network. We have designed the display and analysis software to run on Linux, Windows, or MacOS, to facilitate work upon the same data set by different users, to enable sharing of processing and analysis scripts, and to view lists of events generated by colleagues. Because the entire SCT software package is open source, work done by one group to enhance and extend its performance will become available to other groups at no charge.

Eight weeks of recordings at 512 SPS from eight animals generates over 100 GBytes of data. Efficient methods are therefore required to detect epileptic activity, and to differentiate interictal spikes and seizures from normal brain activity, noise, and other artifacts (White et al., 2006). The SCT system's Neuroarchiver program performs initial processing of the data in real time, or it can process data recorded to disk. Suitable processing will summarize the content of recorded signals for the purpose of analysis. Analysis might calculate the hourly average power in various frequency bands or detect epileptic seizures automatically. Processing 100 GBytes of recordings takes a laptop computer several days, but analyzing the summary data takes less than an hour. Processing and analysis are defined in scripts designed by the experimenter, most likely based upon sample scripts obtained from other experimenters, or from the OSI website. The product of analysis might be a list of epileptic seizures. The Neuroarchiver will read in this list and allow the user to navigate through hundreds of gigabytes of data with the press of a button.

The SCT transmitter's ability to record frequencies greater than 80 Hz with low noise for eight weeks allows us to record the development of fast oscillations during epileptogenesis. High-frequency oscillations in the hippocampal and entorhinal cortical areas are linked to epileptic activity both in humans and in experimental animal models (Bragin et al., 1999; Jacobs et al., 2008; Worrell et al., 2004), and are closely associated with epileptogenesis (Bragin et al., 2004, 2005). During interictal periods, high-frequency cortical activity provides a reliable marker of the primary epileptogenic zone (Jiruska et al., 2010). Such oscillations also occur at frequencies that are beyond the bandwidth of our present device. The transmitter's programmable logic chip and simple design, however, allow it to be modified before encapsulation to provide higher sample rates and thus a broader bandwidth, although at the cost of battery life. In the future, we plan to design transmitters that detect two or more signals, although these extensions will also reduce the battery life.

5. Conclusion

We present a novel telemetric recording system that provides robust and continuous signal monitoring of frequencies up to 160 Hz for at least eight weeks when implanted in live, freely moving rats. The data acquisition and analysis software are open-source, and will perform custom, automatic event detection under the control of the experimenter. All specifications and designs of the system are also open-source and freely available. In principle, it is possible for experimenters to construct the hardware themselves, but the components are available from OpenSource Instruments at what we believe to be a fraction of the cost of competing systems.

References

Betts T. Epilepsy and stress. Br Med J 1992;305:378–9.
Bragin A, Azizyan A, Almajano J, Wilson CL, Engel J. Analysis of chronic seizure onsets after intrahippocampal kainic acid injection in freely moving rats. Epilepsia 2005;46:1592–8.
Bragin A, Engel J, Wilson CL, Fried I, Mathern GW. Hippocampal and entorhinal cortex high-frequency oscillations (100–500 Hz) in human epileptic brain and in kainic acid-treated rats with chronic seizures. Epilepsia 1999;40:127–37.
Bragin A, Wilson CL, Almajano J, Mody I, Engel J. High-frequency oscillations after status epilepticus: epileptogenesis and seizure genesis. Epilepsia 2004;45:1017–23.
Goecke JC, Awad H, Lawson JC, Boivin GP. Evaluating postoperative analgesics in mice using telemetry. Comp Med 2005;55:37–44.
Grabenstatter HL, Ferraro DJ, Williams PA, Chapman PL, Dudek FE. Use of chronic epilepsy models in antiepileptic drug discovery: the effect of topiramate on spontaneous motor seizures in rats with kainate-induced epilepsy. Epilepsia 2005;46:8–14.
Hartikainen K, Rorarius MGF. Cortical responses to auditory stimuli during isoflurane burst suppression anaesthesia. Anaesthesia 1999;54:210–4.

Hernandez EJ, Williams PA, Dudek FE. Effects of fluoxetine and TFMPP on spontaneous seizures in rats with pilocarpine-induced epilepsy. Epilepsia 2002;43:1337–45.
Jacobs J, LeVan P, Chander R, Hall J, Dubeau F, Gotman J. Interictal high-frequency oscillations (80–500 Hz) are an indicator of seizure onset areas independent of spikes in the human epileptic brain. Epilepsia 2008;49:1893–907.
Jiruska P, Finnerty GT, Powell AD, Lofti N, Cmejla R, Jefferys JGR. Epileptic high-frequency network activity in a model of non-lesional temporal lobe epilepsy. Brain 2010;133:1380–90.
Kadam SD, White AM, Staley KJ, Dudek FE. Continuous electroencephalographic monitoring with radio-telemetry in a rat model of perinatal hypoxia-ischemia reveals progressive post-stroke epilepsy. J Neurosci 2010;30:404–15.
Kramer K, Kinter L, Brockway BP, Voss HP, Remie R, Van Zutphen LFM. The use of radiotelemetry in small laboratory animals: recent advances. Contemp Top Lab Anim Sci 2001;40:8–16.
Kwan P, Brodie MJ. Early identification of refractory epilepsy. N Engl J Med 2000;342:314–9.
Lapray D, Bergeler J, Dupont E, Thews O, Luhmann H. A novel miniature telemetric system for recording EEG activity in freely moving rats. J Neurosci Methods 2008;168:119–26.
Lieb JP, Walsh GO, Babb TL, Walter RD, Crandall PH, Tassinari CA, et al. A comparison of EEG seizure patterns recorded with surface and depth electrodes in patients with temporal lobe epilepsy. Epilepsia 1976;17:137–60.
Litt B, Esteller R, Echauz J, D'Alessandro M, Shor R, Henry T, et al. Epileptic seizures may begin hours in advance of clinical onset: a report of five patients. Neuron 2001;30:51–64.
Mumford H, Wetherell JR. A simple method for measuring EEG in freely moving guinea pigs. J Neurosci Methods 2001;107:125–30.
Obeid I, Nicolelis MAL, Wolf PD. A multichannel telemetry system for single unit neural recordings. J Neurosci Methods 2004;133:33–8.
Racine RJ. Modification of seizure activity by electrical stimulation. II. Motor seizure. Electroencephalogr Clin Neurophysiol 1972;32:281–94.
Sander JW, Shorvon SD. Epidemiology of the epilepsies. J Neurol Neurosurg Psychiatry 1996;61:433–43.
Schmidt D, Rogawski MA. New strategies for the identification of drugs to prevent the development or progression of epilepsy. Epilepsy Res 2002;50:71–8.
Swinyard EA, Miyahara JT, Clark LD, Goodman LS. The effect of experimentally-induced stress on pentylenetetrazol seizure threshold in mice. Psychopharmacology (Berl) 1963;4:343–53.
Traub RD, Whittington MA, Buhl EH, LeBeau FEN, Bibbig A, Boyd S, et al. A possible role for gap junctions in generation of very fast EEG oscillations preceding the onset of, and perhaps initiating, seizures. Epilepsia 2001;42:153–70.
Walker MC, White HS, Sander JWAS. Disease modification in partial epilepsy. Brain 2002;125:1937–50.
White AM, Williams PA, Ferraro DJ, Clark S, Kadam SD, Dudek FE, et al. Efficient unsupervised algorithms for the detection of seizures in continuous EEG recordings from rats after brain injury. J Neurosci Methods 2006;152:255–66.
Williams PA, White AM, Ferraro DJ, Clark S, Staley KJ, Dudek FE. The use of radiotelemetry to evaluate electrographic seizures in rats with kainate-induced epilepsy. J Neurosci Methods 2006;155:39–48.
Williams PA, White AM, Clark S, Ferraro DJ, Swiercz W, Staley KJ, et al. Development of spontaneous recurrent seizures after kainate-induced status epilepticus. J Neurosci 2009;29:2103–12.
Wood GE, Young LT, Reagan LP, Chen B, McEwen BS. Stress-induced structural remodeling in hippocampus: prevention by lithium treatment. Proc Natl Acad Sci USA 2004;101:3973–8.
Worrell GA, Parish L, Cranstoun SD, Jonas R, Baltuch G, Litt B. High-frequency oscillations and seizure generation in neocortical epilepsy. Brain 2004;127:1496–506.
Welch BB. Practical programming in Tcl and Tk. 2nd ed. Prentice Hall; June 1997.